00-1097

LA-UR-??-????

Approved for public release;
distribution is unlimited.

Title:	*CRITIQUE OF DUAL CONTINUUM FORMULATIONS OF MULTICOMPONENT REACTIVE TRANSPORT IN FRACTURED POROUS MEDIA*
Author(s):	Peter C. Lichtner (lichtner@lanl.gov)
Submitted to:	Witherspoon International Symposium
Date:	February 29, 2000

DISCLAIMER

TABLE OF CONTENTS

List of Figures

List of Tables

ABSTRACT

Subsurface flow processes may take place at many different scales. The different scales refer to rock pore structure, micro-fractures, distinct fracture networks ranging from small to large fracture spacing, and even faults. Presently, there is no satisfactory methodology for describing quantitatively flow and reactive transport in multi-scale media. Approaches commonly applied to model fractured systems include single continuum models (SCM), equivalent continuum models (ECM), discrete fracture models (DFM), and various forms of dual continuum models (DCM). The SCM describes flow in the fracture network only and is valid in the absence of fracture-matrix interaction. The ECM, on the other hand, requires pervasive interaction between fracture and matrix and is based on averaging their properties. The ECM is characterized by equal fracture and matrix solute concentrations, but generally different mineral concentrations. The DFM is perhaps the most rigorous, but would require inordinate computational resources for a highly fractured rock mass. The DCM represents a fractured porous medium as two interacting continua with one continuum corresponding to the fracture network and the other the matrix. A coupling term provides mass transfer between the two continua. Values for mineral and solute concentrations and other properties such as liquid saturation state may be assigned individually to fracture and matrix. Two forms of the DCM are considered characterized by connected and disconnected matrix blocks. The former is referred to as the DCCM (dual continuum connected matrix) model and the latter as the DCDM (dual continuum disconnected matrix) model. In contrast to the DCCM model in which concentration gradients in the matrix are allowed only parallel to the fracture, the DFM provides for matrix concentration gradients perpendicular to the fracture. The DFM and DCCM models can agree with each other only in the case where both reduce to the ECM. The DCCM model exhibits the incorrect behavior as the matrix block size increases, resulting in reduced coupling between fracture and matrix continua. The DCDM model allows for matrix gradients within individual matrix blocks in which the symmetry of the surrounding fracture geometry is preserved. However, the DCDM model breaks down for simultaneous heat and mass transport and cannot account for significant changes in porosity and permeability caused by chemical reactions.

1 INTRODUCTION

Fractured porous media, and more generally hierarchical media involving multiple length scales, play a ubiquitous role in flow and transport processes in the Earth's subsurface. Fracture dominated flow systems are involved in numerous subsurface geochemical processes including contaminant migration, ore deposition, weathering and others. Practical applications involving fractured porous media include contaminant migration, oil recovery from fractured reservoirs, geothermal energy, degradation of cement, and potentially subsurface sequestration of CO_2, to mention but a few.

Considerable progress has been made in developing and applying reactive transport models to complex geochemical systems involving porous media characterized by a single continuum [see Lichtner et al. (1996) for a general overview and references therein; Lichtner, 1998]. However, subsurface flow processes may take place at many different scales. The different scales refer to rock pore structure, micro-fractures, distinct fracture networks ranging from small to large fracture spacing, and faults. At present there does not exist a completely satisfactory methodology for describing quantitatively reactive flow and transport in multi-scale media.

Because fractured porous media are characterized by bimodal distributions in physical and chemical properties with generally distinct values associated with the fracture network and rock matrix, a description based on a single porous medium is generally unable to capture the unique features characteristic of a fractured system. Furthermore, existing approaches presently used

for describing fracture-matrix interaction are of limited use. This is especially true for transport of chemically reacting constituents and situations where simultaneous flow of mass and heat is involved. A prime example where present approaches may fail and where more general methods are needed is the proposed Yucca Mountain high level nuclear waste repository which is to be hosted in a variably saturated fractured tuff rock. This contribution provides a critical review of existing approaches for representing fractured media in continuum-based models applied to reactive flow and transport. Extension of these methods to hierarchical porous media is considered briefly.

This contribution provides an overview of existing conceptual and numerical methods based on a continuum approach for describing reactive chemical transport in fractured media. The presentation is restricted to continuum-based formulations, in contrast to other approaches such as algorithmic methods including Cellular Automata and Diffusion Limited Aggregation (DLA), and network models, for example. This is because the level of chemistry which can be incorporated into continuum models is on a par with the most sophisticated geochemical models. These models incorporate presently available thermodynamic and kinetic data for complex multicomponent systems. This work reviews previous efforts to describe fracture-matrix interaction involving fluid and heat flow with particular emphasis on the applicability of these methods to reactive chemical transport.

2 CONTINUUM MODELS FOR REACTIVE FLOWS IN FRACTURED MEDIA

A number of different conceptual frameworks have been used to represent fractured porous media. They include the discrete fracture model (DFM), equivalent continuum model (ECM), variations of dual and multiple continuum models (DCM), and the representation of fractures as regions of high permeability-low porosity in heterogeneous media. Incorporation of chemical reactions in models of fractured porous media requires new considerations of the suitability and extension of some of the basic techniques used to represent fluid flow, especially with regard to the appropriate length scale to account for the presence of reaction fronts. Furthermore, because equations for multicomponent systems require a much greater computational effort to solve, new numerical techniques are required. Finally, chemical reactions can dramatically alter the physical and hence flow properties of a porous medium. Fractures may widen or become sealed as a result of chemical reactions. Alteration of the matrix surrounding fractures may affect the interaction between fracture and matrix.

A fractured porous medium is composed of two distinct continua, referred to as fracture and matrix, represented by sub- and super-scripts f and m. A representative elementary volume (REV) of bulk rock with volume V_b consists of the sum of fracture V_f and matrix V_m volumes

$$V_b = V_f + V_m, \tag{2.1}$$

as illustrated in Figure 1. The fraction of volume occupied by fractures, denoted by ϵ_f, is defined by

$$\epsilon_f = \frac{V_f}{V_b}, \tag{2.2}$$

with $\epsilon_m = 1 - \epsilon_f$ representing the fraction occupied by the rock matrix. The fracture and matrix volumes may be further broken down into pore and solid fractions

$$V_\alpha = V_p^\alpha + V_{\text{solid}}^\alpha, \quad (\alpha = f, m), \tag{2.3}$$

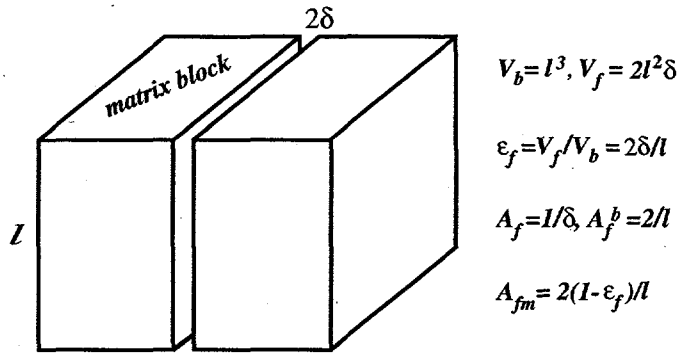

Figure 1: Illustration of geometric relations in a fractured porous medium with fracture aperture 2δ. See text for an explanation of symbols used in the figure.

Note that ϵ_f corresponds to the fracture porosity of the bulk rock volume for the case that the fractures are not filled with solid ($V_p^f = V_f$). In general, however, due to the presence of fracture filling in the form of solids, the intrinsic porosity of the fracture is less than unity. Bulk and intrinsic fracture and matrix properties of some quantity $\mathcal{Z}$ are related by ϵ_α:

$$\mathcal{Z}_\alpha^b = \epsilon_\alpha \mathcal{Z}_\alpha. \tag{2.4}$$

where $\mathcal{Z}_\alpha^b$ denotes the bulk and $\mathcal{Z}_\alpha$ the intrinsic property.

Because of their small aperture and volume, fractures can be easily altered by chemical reactions. To illustrate this effect consider the redistribution of silica between matrix and fracture as heat drives fluid from the matrix into the fracture network. An example of this process might be heat generated by the decay of high level nuclear waste at the proposed Yucca Mountain repository. Imagine that the pore fluid in the rock matrix is brought to equilibrium with respect to a particular silica polymorph such as amorphous silica at boiling conditions. Further consider that as the fluid in the matrix boils it escapes into the surrounding fracture network. As the matrix pore fluid is vaporized, its silica content is deposited in surrounding fractures partially filling the fractures by precipitating silica polymorphs. At issue is the extent to which the fractures can be filled by the silica contained in the matrix pore water. To determine the volume fraction of solid precipitated in the fracture $\phi_{\mathrm{SiO_2}}^f$, the expression

$$\phi_{\mathrm{SiO_2}}^f = \frac{1-\epsilon_f}{\epsilon_f} \phi_m C_{\mathrm{SiO_2}}^m \overline{V}_{\mathrm{SiO_2}}, \tag{2.5}$$

is evaluated, where $C_{\mathrm{SiO_2}}^m$ denotes the concentration of silica in the matrix pore fluid at 100°C assumed to be in equilibrium with a particular silica polymorph with molar volume $\overline{V}_{\mathrm{SiO_2}}$, and matrix porosity ϕ_m. This relation, derived from mass balance considerations, is dependent on all matrix pore water flashing to steam in the fracture. If this is not the case, for example a drying front may propagate inward into the matrix depositing silica within the matrix, then Eqn.(2.5) provides an upper bound on the extent of fracture filling. Other processes may also be possible, such as silica becoming remobilized from fracture coatings, which are not accounted for in this simple analysis. Results for a matrix porosity of $\phi_m = 0.1$ are shown in Figure 2 for quartz, chalcedony and amorphous silica. From the figure it is clear that for a given matrix porosity, the degree of sealing of the fracture depends on the fracture volume fraction ϵ_f and the particular silica polymorph which precipitates. Amorphous silica with a higher solubility gives the largest fracture filling followed by chalcedony and quartz. For complete sealing of the fracture ($\phi_{\mathrm{SiO_2}}^f = 1$) a very small fracture volume fraction is necessary. Moderate filling could lead to fracture coatings that armor the fracture and prevent or reduce imbibition into the matrix. Thus very different consequences could result depending on the extent of fracture filling.

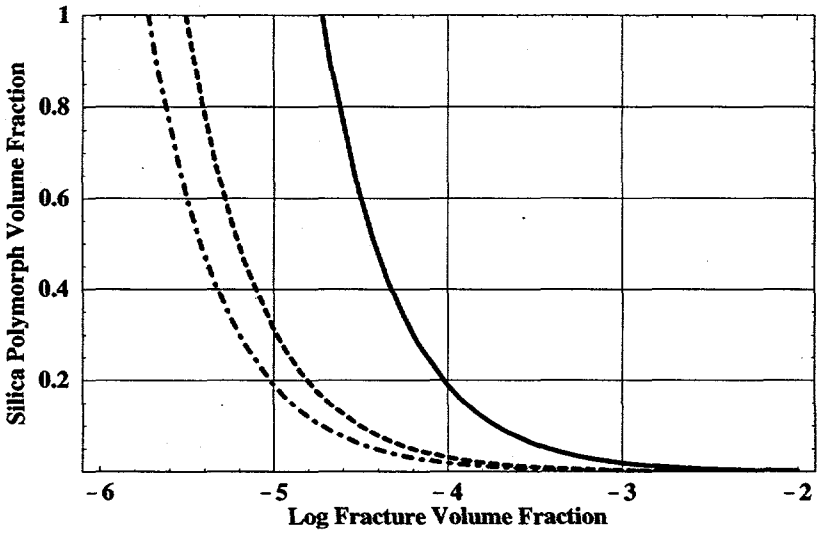

Figure 2: Volume fraction of quartz (solid curve), chalcedony (dashed curve) and amorphous silica (dash-dotted curve) plotted as a function of fracture porosity. A volume fraction of one represents complete filling of the fracture assuming that the fracture was initially devoid of solid filling.

This example is but a highly simplified situation that could take place at the proposed Yucca Mountain nuclear waste facility. Heat from the waste is expected to lead to the formation of heat pipes with consequent boiling and degassing of CO_2 with an increase in pH and possible precipitation of salts as evaporation takes place (Lichtner and Seth, 1996).

2.1 Discrete Fracture Model (DFM)

One approach is to treat fractures explicitly taking into account coupling with the rock matrix through a mass transfer term (Figure 3). This approach, referred to as the discrete fracture model (DFM), applies to a single fracture or an infinite number of equally spaced fractures. The DFM, however, rapidly becomes unwieldy for more than a few fractures if there is no simple geometric relation between them.

Several forms of the DFM are possible depending on treatment of transport processes in the fracture and matrix. Here a simplified form for the solute transport equations is considered neglecting diffusion in the fracture and advection and diffusion parallel to the fracture in the matrix. This is a good approximation for sufficiently fast flow rates in the fracture. A single reacting species is considered obeying the reaction

$$\mathcal{A} \rightleftharpoons \mathcal{A}_{(s)}, \tag{2.6}$$

with solid $\mathcal{A}_{(s)}$ and aqueous species $\mathcal{A}$. Transport equations for the DFM can be expressed as

$$\frac{\partial}{\partial t}(\phi_f C_f) + v_f \frac{\partial C_f}{\partial z} = -k_f(C_f - C_{\rm eq}) + \frac{\tau_m \phi_m D}{\delta} \frac{\partial C_m}{\partial x}\bigg|_{x=\delta}, \tag{2.7}$$

for the fracture, and

$$\frac{\partial}{\partial t}(\phi_m C_m) + v_m \frac{\partial C_m}{\partial x} - \tau_m \phi_m D \frac{\partial^2 C_m}{\partial x^2} = -k_m(C_m - C_{\rm eq}), \tag{2.8}$$

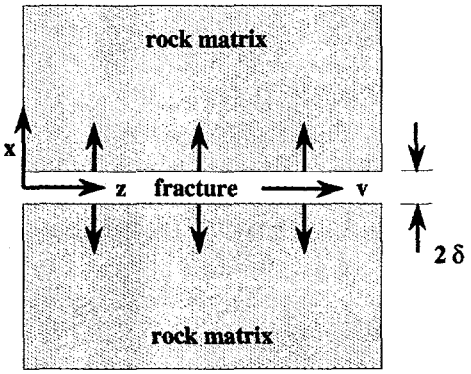

Figure 3: Discrete fracture model.

for the matrix, where z is the coordinate along the fracture, and x is the coordinate in the matrix perpendicular to the fracture. Linear reaction kinetics are assumed with rate constants k_f and k_m for fracture and matrix, respectively, and equilibrium concentration $C_{\rm eq}$. The solute concentration is denoted by C_α ($\alpha = f,\, m$), corresponding to fracture and matrix. Diffusivity is denoted by D, and fracture and matrix porosity and tortuosity by τ_α and ϕ_α, respectively. The fluid flow velocity in the fracture and matrix is represented by v_f and v_m, respectively. To complete the set of equations initial and boundary conditions must be prescribed. At the fracture-matrix interface the solute concentrations are presumed to be the same

$$C_m(x = \delta,\, z) \;=\; C_f(z). \tag{2.9}$$

The fracture transport equation is coupled to the matrix equation by the last term on the right-hand side of Eqn.(2.7) representing the flux across the fracture-matrix interface.

Recently, Steefel and Lichtner (1998a,b) demonstrated a unique relation between mineral alteration along a fracture and that within the rock matrix perpendicular to the fracture. This property can be investigated by examining the stationary state solution to the DFM transport equations. The stationary state solution is useful for describing the time evolution of a reacting system which may be represented as a sequence of stationary states, with each stationary state corresponding to a different configuration of minerals along the flow path (Lichtner, 1988). The stationary state solution to the DFM transport equations can be expressed as (Steefel and Lichtner, 1998a)

$$C_f(z) = \left(C_f^0 - C_{\rm eq}\right) {\rm e}^{-z/\lambda_f} + C_{\rm eq}, \tag{2.10}$$

and

$$C_m(x;\, z) = \Big(C_f(z) - C_{\rm eq}\Big) {\rm e}^{-x/\lambda_m} + C_{\rm eq}, \tag{2.11}$$

where $\lambda_{m,\,f}$ represent equilibration lengths (Lichtner, 1988; 1998) in the fracture and matrix, respectively, defined by

$$\lambda_m = \sqrt{\frac{(\tau\phi D)_m}{k_m}}, \tag{2.12}$$

$$\lambda_f = \frac{{\rm Pe}\lambda_f^0 \lambda_m}{\lambda_f^0 + {\rm Pe}\lambda_m}, \tag{2.13}$$

where the dimensionless Peclet-like number Pe is defined by

$$\mathrm{Pe} = \frac{v_f \delta}{(\tau \phi D)_m}. \tag{2.14}$$

and where $\lambda_f^0 = v_f / k_f$ denotes the fracture equilibration length for pure advective transport (Lichtner, 1988). According to these results a wedge-shaped front geometry is produced with slope

$$\frac{dx}{dz} = -\frac{\lambda_m}{\lambda_f} = -\left(\frac{1}{\mathrm{Pe}} + \frac{\lambda_m}{\lambda_f^0}\right). \tag{2.15}$$

The slope is characterized by the sum of the two dimensionless groups Pe and λ_m/λ_f^0. A simple scaling relation exists between the concentration profile into the rock matrix C_m and along the fracture C_f of the form

$$C_m(x, z) = C_f\left(\frac{\lambda_f}{\lambda_m} x + z\right). \tag{2.16}$$

Similar scaling relations hold for other quantities such as reaction rates and mineral concentrations. Numerical analysis involving multicomponent systems with nonlinear reaction kinetics yielded similar results.

A surprising result of this analysis is that in spite of the high flow velocity in the fracture, with only diffusive transport in the matrix, the fracture behaves as a diffusion dominated system because of the strong interaction with the matrix (Steefel and Lichtner, 1998). The results suggest that field observations of matrix alteration perpendicular to the fracture may be used to predict mineralization along the fracture itself. How well this prediction is born out in natural systems depends on strong communication between the fracture and matrix that could be significantly impeded by the presence of impermeable fracture coatings, for example.

These results may be generalized to include an infinite set of equally spaced fractures with spacing d (Lichtner, 1998). In this case the stationary state matrix solute concentration is given by

$$C_m(x; z) = \left(C_f(z) - C_{\mathrm{eq}}\right) \frac{\cosh\left[\dfrac{x - d/2}{\lambda_m}\right]}{\cosh\left[\dfrac{\delta - d/2}{\lambda_m}\right]} + C_{\mathrm{eq}}. \tag{2.17}$$

This solution reduces to the previous case of infinite fracture spacing for $d \gg \lambda_m \gg \delta$. For finite fracture spacing which is small compared to the matrix equilibration length, the scaling relation between fracture and matrix concentration profiles no longer holds. If the fracture spacing is much smaller compared to the matrix equilibration length ($\delta \ll d \ll \lambda_m$), matrix concentration gradients disappear and the solute concentration in the fracture and matrix become equal. This is just the definition of the ECM which is a limiting case of the DFM.

2.2 Dual Continuum Models: DCCM & DCDM Approaches

The dual continuum model (DCM) represents a fractured porous medium as two interacting continua with one continuum corresponding to the fracture network and the other the matrix. A coupling term provides mass transfer between the two continua. The fracture continuum is characterized by high permeability and low porosity compared to the matrix continuum. The DCM enables

separate values of the field variables to be assigned to fracture and matrix continua. Additional parameters are needed to represent the average matrix block size and fracture aperture, or equivalently fracture volume, associated with a representative elemental volume (REV) of bulk medium. From these geometric quantities the interfacial surface area between fracture and matrix can be computed.

In the field of reservoir engineering dual continuum models have been in use for some time since their first introduction by Barenblatt and Zheltov (1960) and Barenblatt et al. (1960). The approach put forth by Barenblatt and Zheltov (1960) represented a fractured reservoir as two distinct overlapping continua. Flow equations were developed for each continuum, with a coupling term providing mass transfer between them. Shortly thereafter, Warren and Root (1963) published an alternative conceptual model in which the matrix was represented as a periodic array of identical blocks completely surrounded by fractures. Pruess and Narisimhan (1985) generalized the approach of Warren and Root (1963) to include multiple nodes within a matrix block allowing for local gradients to be present within the rock matrix. These authors also provided for a fully transient description. In this approach the matrix is discretized into concentrically nested blocks, spheres, or other geometric shapes. The outer most block is connected to the fracture continuum. The authors referred to their generalization as the so-called MINC (Multiple Interacting Continuum) approach. The term MINC, however, is somewhat of a misnomer. In their original paper, Pruess and Narisimhan (1985) associated different continua with the grid, and not as a material property of the medium independent of the grid. In so far as the matrix is considered as a single continuum in which provision is made for gradients in various field variables such as pressure, temperature, saturation, concentration etc., there are still only two solid continua—fracture and matrix, rather than "multiple" continua.

The two distinct approaches to formulating dual continuum models may be conveniently distinguished by the connectivity of the rock matrix (the fracture is always considered to be connected in the following). In the case of Barenblatt and Zheltov (1960), the matrix continuum is completely connected with each matrix block connected to its neighboring blocks. In contrast, for the conceptual model used by Warren and Root (1963) and Pruess and Narisimhan (1985), the matrix continuum is disconnected with each matrix block connected to surrounding fractures, but not to other matrix blocks. In what follows these two approaches are referred to as the dual continuum connected matrix (DCCM) and dual continuum disconnected matrix (DCDM) formulations of the DCM. As originally formulated, the DCCM model associates a single matrix node with each fracture node. This turns out to be a distinct disadvantage of the DCCM approach since it does not allow for gradients within the matrix perpendicular to the fracture. An extension of the DCCM formulation to include more than one matrix node for each fracture node has been used, but only to limited extent. The computer code FEHM (Zyvoloski et al., 1997), for example, allows for the possibility of two matrix nodes for each fracture node. This extension of the DCCM model to multiple matrix nodes is referred to as the MDCCM model, or Multiple Node Dual Continuum Connected Matrix model. The structure of the MDCCM model is similar in many respects to the DFM, with the transport equation for the discrete fracture replaced by a continuum formulation. As a consequence it would have similar computational requirements as the DFM. The MDCCM model is not considered further in this critique.

It is not clear that dual continuum models can provide sufficient flexibility, especially in the case of sufficiently fast chemical reactions where the equilibration length is on the order of the pore scale or microscale. In such cases a hierarchical approach may be needed. "Fast" heterogeneous reactions have often in the past been represented by local equilibrium. However, in fact, such reactions may be much more complicated than surface controlled kinetic reactions because they may result in local concentration gradients and hence become sensitive to pore and fracture geometry. An important unanswered question is how to scale such processes to the macroscale where the continuum formulation is valid. Triple- and multiple-porosity models that have been used to

Table 1: Summary of acronyms used for continuum models describing flow and transport in fractured porous media and their definitions.

Model	Definition	Description
SCM	Single Continuum Model	Fracture can be represented as a single continuum with no interaction with the matrix
ECM	Equivalent Continuum Model	Pervasive interaction between fracture and matrix
DFM	Discrete Fracture Model	Applicable to sparse, widely spaced fractures
DCM	Dual Continuum Model	Representation of fracture and matrix as separate continua
DCCM	Dual Continuum Connected Matrix	DCM in which matrix continuum is connected and discretized by a single node
MDCCM	Multiple Node Dual Continuum Connected Matrix	DCM in which matrix continuum is connected and discretized by multiple nodes
DCDM	Dual Continuum Disconnected Matrix	DCM in which matrix continuum is disconnected

describe flow through fractured porous media (Closmann, 1975; Abdassah and Ershaghi, 1986; Chen, 1989) may be useful in such instances, but are beyond the scope of the present treatment.

Terminology is not applied consistently in the literature when referring to these two different conceptual approaches. Barenblatt et al. (1960) used the terminology double porosity. However, other authors since then have attempted to distinguish the cases of a connected and disconnected matrix continuum as dual permeability (Barenblatt and Zheltov, 1960) versus dual (or double) porosity (Warren and Root, 1963) models, respectively. Hill and Thomas (1985) generalized the dual porosity model to include arbitrary connectivity referred to as a dual permeability–dual porosity model. Triple porosity models have also been considered (Bai et al., 1993). To confuse the issue, in the soil literature the connected matrix continuum approach is referred to as a double porosity model (Gerke and Van Genuchten, 1993; Chittaranjan et al., 1997), rather than dual permeability as is common in the oil reservoir literature. A summary of the acronyms and their definitions used here are listed in Table 1.

2.2.1 Dual Continuum Connected Matrix (DCCM) Model

The DCCM formulation represents the fracture network and matrix as distinct but coexisting continua. A coupling term provides exchange of mass and heat between the two continua. In what follows a multicomponent chemically reacting system consisting of N aqueous species and M minerals is considered. Homogeneous reactions within the aqueous phase and mineral precipitation/dissolution reactions take place represented by the reactions

$$\sum_j \nu_{ji} \mathrm{A}_j \rightleftharpoons \mathrm{A}_i, \quad \sum_j \nu_{js} \mathrm{A}_j \rightleftharpoons \mathrm{M}_s, \tag{2.18}$$

written in terms of a set of (nonunique) aqueous primary or basis species A_j, aqueous secondary species A_i, and minerals M_s. The quantities ν_{ji} and ν_{js} represent the stoichiometric reaction coefficients. These reactions take place simultaneously in the fracture and matrix continua. Homogeneous reactions are presumed to be sufficiently fast allowing for a local equilibrium description.

Ion exchange and surface complexation reactions are not considered in the present treatment, although they are straightforward to include. Mass conservation equations for a multicomponent system for fracture and matrix continua can be written in the form

$$\frac{\partial}{\partial t}\left(\epsilon_f \phi_f \Psi_j^f\right) + \boldsymbol{\nabla}\cdot\epsilon_f \boldsymbol{\Omega}_j^f = -\epsilon_f \sum_s \nu_{js} I_s^f - \Gamma_j^{fm}, \tag{2.19}$$

for the fracture continuum, and for the matrix continuum as

$$\frac{\partial}{\partial t}\left(\epsilon_m \phi_m \Psi_j^m\right) + \boldsymbol{\nabla}\cdot\epsilon_m \boldsymbol{\Omega}_j^m = -\epsilon_m \sum_s \nu_{js} I_s^m + \Gamma_j^{fm}, \tag{2.20}$$

for aqueous primary species labeled j, and for minerals as

$$\frac{\partial \phi_s^\alpha}{\partial t} = \overline{V}_s I_s^\alpha, \quad (\alpha = f, m). \tag{2.21}$$

These equations are referenced to the bulk rock REV. For simplicity a fully saturated system is considered. The quantities ϕ_α, ϕ_s^α, Ψ_j^α, $\boldsymbol{\Omega}_j^\alpha$, and I_s^α, $(\alpha = f, m)$ refer to intrinsic fracture and matrix properties corresponding to porosity, mineral volume fraction, total solute concentration and flux, and mineral reaction rate, respectively. The quantity $\overline{V}_s$ denotes the mineral molar volume. The total concentration Ψ_j^α is defined relative to an arbitrarily chosen set of primary species with concentrations C_j^α as

$$\Psi_j^\alpha = C_j^\alpha + \sum_i \nu_{ji} C_i^\alpha, \quad C_i^\alpha = (\gamma_i^\alpha)^{-1} K_i \prod_j \left(\gamma_j^\alpha C_j^\alpha\right)^{\nu_{ji}}, \tag{2.22}$$

where C_i^α denotes the concentration of the ith secondary species derived from the primary species concentrations through mass action equations with equilibrium constant K_i and activity coefficients $\gamma_{i,j}$ [see Lichtner et al. (1996) for more details]. The solute flux consisting of contributions from advection, dispersion and molecular diffusion is defined by

$$\boldsymbol{\Omega}_j^\alpha = -\tau_\alpha \phi_\alpha D_\alpha \boldsymbol{\nabla}\Psi_j^\alpha + \boldsymbol{v}_\alpha \Psi_j^\alpha, \quad (\alpha = f, m), \tag{2.23}$$

with tortuosity τ_α and diffusion coefficient D_α assumed to be the same for all species within each continuum. The mineral kinetic reaction rate I_s^α can be expressed as a sum over various parallel reaction mechanisms which has the general form based on transition state theory

$$I_s^\alpha = -\mathcal{A}_s^\alpha \sum_l k_{sl} \mathcal{P}_{sl}^\alpha \left[1 - (K_{sl} \mathcal{Q}_{sl}^\alpha)^{1/\sigma_{sl}}\right], \tag{2.24}$$

with kinetic rate constant k_{sl}, mineral surface area $\mathcal{A}_s^\alpha$, equilibrium constant $K_{sl}(T,p)$, Tempkin constant σ_{sl}, and prefactor $\mathcal{P}_{sl}^\alpha$ consisting of products of primary and secondary species concentrations raised to respective powers n_{js} and n_{is} (Lichtner, 1998)

$$\mathcal{P}_{sl}^\alpha = \prod_j a_j^{n_{js}^l} \prod_i a_i^{n_{is}^l}. \tag{2.25}$$

The ion activity product $\mathcal{Q}_{sl}^\alpha$ is defined as

$$\mathcal{Q}_{sl}^\alpha = \prod_j a_j^{\nu_{js}^l}. \tag{2.26}$$

The surface area $\mathcal{A}_s^\alpha$ is in general different for each continuum, and as a consequence so also is the reaction rate I_s^α even in the limiting case of equal fracture and matrix aqueous concentrations.

The coupling term Γ_j^{fm} is equal to the product of the interfacial specific surface area $\mathcal{A}_{fm}$ between fracture and matrix continua multiplied by the flux Ω_j^{fm} between fracture and matrix defined by

$$\Gamma_j^{fm} = \mathcal{A}_{fm}\Omega_j^{fm}. \tag{2.27}$$

For the geometry shown in Figure 1, the interfacial specific fracture-matrix area $\mathcal{A}_{fm}$ is given by the expression

$$\mathcal{A}_{fm} = \frac{2}{l}(1-\epsilon_f). \tag{2.28}$$

More complex geometries can also be represented leading to more complicated expression for the fracture-matrix surface area.

The aqueous and mineral mass conservation equations are coupled to one another through the reaction rate term, and through changes in porosity, tortuosity, and permeability caused by chemical reactions. The latter effects are more difficult to incorporate into the conservation equations, requiring various phenomenological relations that relate changes in physical continuum properties to changes in mineral concentrations. One approach that is often used is to relate porosity and mineral volume fractions for each continuum by the assumption that they add to unity

$$\phi_\alpha + \sum_s \phi_s^\alpha = 1. \tag{2.29}$$

This relation, however, presupposes that the connected porosity and total porosity are equivalent. Other continuum properties such as permeability and tortuosity are then related to porosity through Archie's law and the Carmen-Kozeny equation, for example. How successful this approach really is needs to be tested in the field and in laboratory experiments.

2.2.2 Dual Continuum Disconnected Matrix (DCDM) Model

An alternative formulation to the DCCM approach that alleviates the limitation to small matrix blocks is the dual continuum disconnected matrix (DCDM) approach. In this approach it is assumed that each matrix block is completely surrounded by fractures (Figure 4). Different matrix blocks can only communicate with one another through the fracture network. In the DCDM formulation, the matrix is resolved into a set of nested rectangular or spherical regions forming an onionskin-like nodal structure. Gradients across a single matrix block, caused by gravity, or thermal or concentration gradients, for example, are thus not possible to describe in this formulation.

Mass transport equations for the DCDM model for fracture continuum have the following form

$$\frac{\partial}{\partial t}\left(\epsilon_f\phi_f\Psi_j^f\right) + \nabla\cdot\left(\epsilon_f\Omega_j^f\right) = -\epsilon_f\sum_s \nu_{js}I_s^f - \Gamma_j^{fm}. \tag{2.30}$$

This equation may be of 1, 2, or 3 spatial dimensions. The matrix continuum transport equations, however, have the one-dimensional form

$$\frac{\partial}{\partial t}\left(\epsilon_m\phi_m\Psi_j^m\right) + \frac{\partial}{\partial y}\left(\epsilon_m\Omega_j^m\right) = -\epsilon_m\sum_s \nu_{js}I_s^m + \Gamma_j^{fm}, \tag{2.31}$$

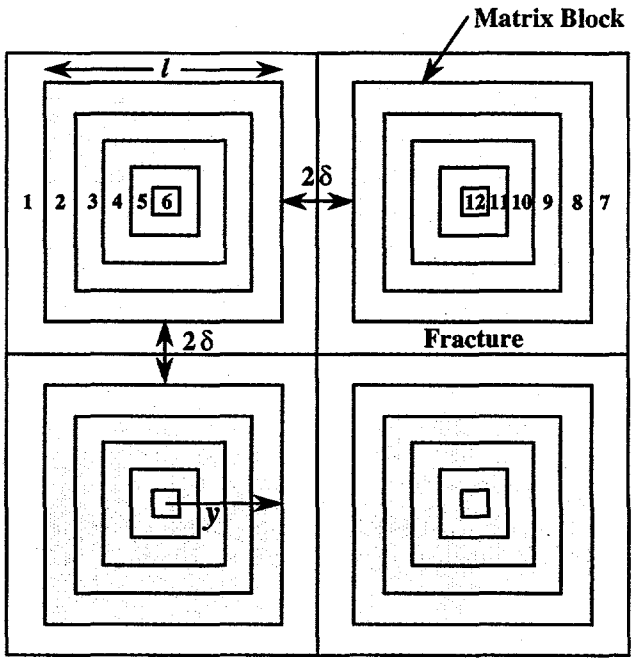

Figure 4: Geometry for the DCDM model for matrix blocks of size l and fracture aperture 2δ indicating the 1D coordinate $\mathcal{Y}$ for each matrix block and possible node numbering scheme.

written with generalized coordinate $\mathcal{Y}$ representing the distance from the fracture to a point within the matrix. The coordinate $\mathcal{Y}$, for example, is a radial coordinate in the case of nested spheres or linear distance for a nested set of cubes. The fracture-matrix coupling term Γ_j^{fm} has the same form as given in Eqn.(2.27) for the DCCM formulation.

Fundamental difficulties occur when applying the DCDM approach to simultaneous heat and mass transport. This may be seen by considering a stack of matrix blocks with each block surrounded by a fracture. The top and bottom of the stack is held at different fixed temperatures. In the absence of heat sources or sinks within the matrix blocks, it is clear that at steady-state conditions temperature gradients cannot exist within the matrix blocks. In fact, for steady state conditions, the temperature of each matrix block must be the same as its surrounding fracture. As a consequence, heat conduction takes place through the fracture network only and not through the matrix blocks. This leads to an effective thermal conductivity determined by the fracture network $\kappa_{\text{eff}} = \kappa_f$. By contrast in a layered medium with layer thicknesses l_i of alternating fracture and matrix properties the effective thermal conductivity is given by the harmonic mean

$$\kappa_{\text{eff}} = \frac{\sum l_i}{\sum \frac{l_i}{\kappa_i}} = \frac{l + 2\delta}{\frac{2\delta}{\kappa_f} + \frac{l}{\kappa_m}} \simeq \kappa_m, \tag{2.32}$$

for $l \gg \delta$, and $k_m \ll k_f$, with half-fracture aperture δ and matrix block size l. Field observations suggest that heat conduction in a fractured porous medium is determined primarily by the matrix conductivity and not the conductivity of the fracture network which above the watertable may be filled primarily with air. Presumably this is because matrix blocks are not completely isolated from each other by fractures, but in fact are in direct contact over some fraction of the fracture interfacial area as a result of asperities and in situ stress field. Thus the DCDM approach gives an incorrect value for the effective thermal conductivity for a composite medium such as a fractured porous rock.

There are other limitations to the DCDM approach as formulated here. It is restricted to a

homogeneous matrix and cannot handle strong changes in porosity and permeability which would alter the flow characteristics of the rock from a fracture dominated system to one of porous flow, a common occurrence in chemical weathering for example (Odling and Roden, 1997). A heterogeneous matrix block would break the symmetry of the nested matrix node structure. Significant changes in porosity and permeability can alter the physical properties of the porous medium altogether. Thus during chemical weathering of a granitic rock, in the extreme case of formation of a bauxite deposit the weathering profile changes continuously with depth from a lateritic layer near the surface containing aluminum oxide ore, to a highly weathered saprolite zone containing clay minerals, to the unweathered granite basement rock. The lateritic and saprolite layers are highly porous and have lost the fracture characteristics of the granite rock mass. The DCDM formulation, for example, could not describe the continuous changes in material properties taking place with depth. As the medium becomes more porous and the fracture properties of the granite rock body are obliterated, the DCDM model would continue to impose a relic symmetry on the medium corresponding to the initial fracture geometry that would not be correct. Moreover, the boundary between the two distinct media in the case of weathering is continuously changing, albeit slowly, with time. The question of continuously joining a non-fractured porous medium to a fractured medium needs more study.

2.3 Equivalent Continuum Model (ECM)

The ECM representation of a fractured porous medium is based on a composite medium obtained by suitably averaging fracture and matrix properties. Concentrations of dissolved constituents are identical in the fracture and matrix. However, mineral concentrations and reaction rates may be, and generally are, distinct in each continuum. As is demonstrated quite generally below through scaling relations, the ECM represents the asymptotic limit of the DCCM model.

2.3.1 Derivation of the ECM from the DCCM Model

For conditions of sufficiently strong fracture-matrix coupling the DCCM model reduces to the ECM. This may be seen by adding Eqns.(2.19) and (2.20) for fracture and matrix aqueous primary species. The fracture-matrix coupling term Γ_j^{fm} drops out yielding the single equation

$$\frac{\partial}{\partial t}\left(\epsilon_f\phi_f\Psi_j^f + \epsilon_m\phi_m\Psi_j^m\right) + \boldsymbol{\nabla}\cdot\left[\epsilon_f\boldsymbol{\Omega}_j^f + \epsilon_m\boldsymbol{\Omega}_j^m\right] = -\sum_s \nu_{js}\left(\epsilon_f I_s^f + \epsilon_m I_s^m\right). \tag{2.33}$$

This equation reduces to the ECM provided that the primary species concentrations in the fracture and matrix are identical

$$C_j^f = C_j^m = C_j^{\rm ecm}. \tag{2.34}$$

In that case, $\Psi_j^{\rm ecm} = \Psi_j^f = \Psi_j^m$, and the accumulation term becomes

$$\epsilon_f\phi_f\Psi_j^f + \epsilon_m\phi_m\Psi_j^m = \phi_{\rm ecm}\Psi_j^{\rm ecm}, \tag{2.35}$$

where the ECM porosity $\phi_{\rm ecm}$ is defined as an average over fracture and matrix porosities

$$\phi_{\rm ecm} = \epsilon_f\phi_f + \epsilon_m\phi_m. \tag{2.36}$$

Likewise, the solute flux reduces to an expression involving the ECM solute concentrations

$$\Omega_j^{\rm ecm} = \epsilon_f \Omega_j^f + \epsilon_m \Omega_j^m = -\tau_{\rm ecm}\phi_{\rm ecm} D \nabla \Psi_j^{\rm ecm} + \boldsymbol{q}_{\rm ecm}\Psi_j^{\rm ecm}. \tag{2.37}$$

In this equation the ECM tortuosity is related to intrinsic fracture and matrix properties by the expression

$$\tau_{\rm ecm} = \frac{\epsilon_f \tau_f \phi_f + \epsilon_m \tau_m \phi_m}{\phi_{\rm ecm}}, \tag{2.38}$$

and the Darcy flux $\boldsymbol{q}_{\rm ecm}$ is given by the weighted sum of intrinsic fracture and matrix velocities

$$\boldsymbol{q}_{\rm ecm} = \epsilon_f \boldsymbol{v}_f + \epsilon_m \boldsymbol{v}_m. \tag{2.39}$$

For equal fracture and matrix concentrations, the mineral reaction rate reduces to

$$I_s^{\rm ecm} = \epsilon_f I_s^f + \epsilon_m I_s^m = -\mathcal{A}_s^{\rm ecm} \sum_l k_{sl} \mathcal{P}_{sl}^{\rm ecm} \left[1 - (K_{sl}\mathcal{Q}_{sl}^{\rm ecm})^{1/\sigma_{sl}}\right], \tag{2.40}$$

where the ECM mineral surface area $\mathcal{A}_s^{\rm ecm}$ is given by the weighted sum of intrinsic fracture and matrix surface areas

$$\mathcal{A}_s^{\rm ecm} = \epsilon_f \mathcal{A}_s^f + \epsilon_m \mathcal{A}_s^m. \tag{2.41}$$

In contrast to the ECM transport equations for solute species, the ECM equations for minerals generally can not be reduced to a single bulk averaged equation. Formally, mineral mass transfer equations for the ECM can be derived that have the same form as the individual fracture and matrix continua given by Eqn.(2.21)

$$\frac{\partial \phi_s^{\rm ecm}}{\partial t} = \overline{V}_s I_s^{\rm ecm}, \tag{2.42}$$

obtained by a weighted sum of Eqn.(2.21) written for fracture and matrix with weight factors ϵ_f and ϵ_m. The mineral volume fraction $\phi_s^{\rm ecm}$ in the ECM formulation is related to the intrinsic fracture and matrix volume fractions by the expression

$$\phi_s^{\rm ecm} = \epsilon_f \phi_s^f + \epsilon_m \phi_s^m. \tag{2.43}$$

The ECM porosity and mineral volume fractions satisfy the relation

$$\phi_{\rm ecm} + \sum_s \phi_s^{\rm ecm} = 1. \tag{2.44}$$

However, unlike solute concentrations, mineral concentrations in the ECM need not be, and generally are not, equal for fracture and matrix. This is because different mineral surface areas apply to each continuum that, furthermore, may change differently with time as reaction progresses. For example, fracture and matrix mineral surface areas may vary with reaction with distinctly different dependencies on mineral volume fraction according to a relation of the form

$$\mathcal{A}_s^\alpha = \mathcal{A}_s^{\alpha 0}\left(\frac{\phi_s^\alpha}{\phi_s^{\alpha 0}}\right)^{n_\alpha}, \tag{2.45}$$

where n_α is a constant which may be different for each continuum. One possible choice for the initial specific mineral surface area in the matrix is to assume the surface area is inversely proportional to mineral grain size and directly proportional to the initial matrix mineral concentration

$$\mathcal{A}_s^{m0} = \frac{\phi_s^{m0}}{b_s^m}. \tag{2.46}$$

The initial fracture mineral specific surface generally has a different value, for example, proportional to the reciprocal of the half-fracture aperture δ for minerals located at the fracture wall, plus the ratio of initial fracture mineral concentration to grain size for fracture filling minerals

$$\mathcal{A}_s^{f0} = \frac{1}{\delta} + \frac{\phi_s^{f0}}{b_s^f}. \tag{2.47}$$

The different mineral surface areas associated with each continuum lead to different reaction rates in fracture and matrix continua, and hence different mineral concentrations even though the solute concentrations are the same for each continuum. For $n_\alpha \neq 0$, mineral volume fractions must be obtained directly from the individual mass transfer equations for fracture and matrix continua through Eqn.(2.21) and not the ECM Eqn.(2.43). This is because it is not possible to express the ECM surface area as defined by Eqn.(2.41) as a function of the ECM mineral volume fraction. It should be noted that it is tacitly assumed that ϵ_f remains constant for all time which need not actually be the case.

Deciding what values to use for the reacting mineral surface areas is perhaps one of the most uncertain parameters to determine. What makes specification of this parameter most difficult is that it is the hydrologically accessible surface area, that is the area that is in contact with the fluid, that is of interest. For accurate determination of the surface, *in situ* experiments and direct field measurements are required.

A consequence of averaging fracture and matrix properties in the ECM is that travel times of non-reacting tracer species are generally longer in the ECM compared to the other models describing transport in fractured media. Indeed, it follows that the ECM travel time for a tracer is given by

$$t_{\rm ecm} = \frac{\phi_{\rm ecm} L}{q_{\rm ecm}}, \tag{2.48}$$

where L denotes the system length. Substituting for $\phi_{\rm ecm}$ and $q_{\rm ecm}$ in terms of their intrinsic fracture and matrix properties gives for the case of flow in the fracture network only ($v_m = 0$)

$$t_{\rm ecm} = \left(1 + \frac{\epsilon_m \phi_m}{\epsilon_f \phi_f}\right) t_f, \tag{2.49}$$

where the fracture travel time t_f is defined as

$$t_f = \frac{\phi_f L}{v_f}. \tag{2.50}$$

The travel time t_f applies to single and dual continuum formulations for the case when flow is absent in the matrix. As a consequence of Eqn.(2.49), the ECM is not conservative in predicting contaminant arrival times in the case of fracture dominated flow.

2.3.2 Asymptotic limit of the DCCM Model: Scaling Relations

As demonstrated by Lichtner (1993) through scaling relations, the reactive mass transport equations based on a kinetic description of mineral reaction rates approach asymptotically the local chemical equilibrium limit. This asymptotic relation between a kinetic description and local equilibrium one provides an immediate understanding for the conditions of validity of local equilibrium. In addition, because the solution to the local equilibrium form of the reactive transport equations can be reduced to solving a set of algebraic equations, this relation also provides a way of checking the accuracy of the more complicated solution to the partial differential equations representing the kinetic formulation. The same considerations apply to the relationship between the DCCM formulation and the ECM. Applying the scaling transformation

$$\boldsymbol{r}_\sigma = \sigma^{-1}\boldsymbol{r}, \tag{2.51}$$

$$t_\sigma = \sigma^{-1}t, \tag{2.52}$$

with constant scale factor σ to the DCCM equations [Eqns.(2.19) and (2.20)] leads to the transformed equations

$$\frac{\partial}{\partial t_\sigma}\left(\epsilon_\alpha\phi_\alpha\Psi_j^\alpha\right) + \boldsymbol{\nabla}_\sigma\cdot\epsilon_\alpha\boldsymbol{\Omega}_{j\sigma}^\alpha = -\sigma\epsilon_\alpha\sum_s \nu_{js}I_s^\alpha + \sigma(1-2\delta_{f\alpha})\Gamma_j^{fm}, \quad (\alpha = f,\, m), \tag{2.53}$$

and

$$\frac{\partial\phi_s^\alpha}{\partial t_\sigma} = \sigma\overline{V}_s I_s^\alpha, \quad (\alpha = f,\, m), \tag{2.54}$$

where the transformed flux $\boldsymbol{\Omega}_{j\sigma}^\alpha$ is given by

$$\boldsymbol{\Omega}_{j\sigma}^\alpha = -\sigma^{-1}(\tau\phi D)_\alpha\boldsymbol{\nabla}_\sigma\Psi_j^\alpha + \boldsymbol{q}_\alpha\Psi_j^\alpha, \tag{2.55}$$

in which the diffusion/dispersion term is scaled, and $\boldsymbol{\nabla}_\sigma$ represents the gradient operator with respect to the scaled spatial coordinates. As a consequence, assuming that the boundary conditions imposed on the system are scale invariant, it follows that the solution to the solute and mineral conservation equations represented by the function $\mathcal{F}(\boldsymbol{r},\, t|\{k\},\, D,\, \boldsymbol{q},\, \mathcal{A}_{fm})$ scales according to the relation

$$\mathcal{F}(\sigma\boldsymbol{r},\, \sigma t|\{k\},\, D,\, \boldsymbol{q},\, \mathcal{A}_{fm}) = \mathcal{F}(\boldsymbol{r},\, t|\sigma\{k\},\, \sigma^{-1}D,\, \boldsymbol{q},\, \sigma\mathcal{A}_{fm}). \tag{2.56}$$

Taking the limit of this relation as $\sigma\to\infty$ leads to the pure advective, local equilibrium form of the ECM as the asymptotic limit of the DCCM equations.

3 DFM–DCCM MODEL COMPARISON

In this section a comparison is made between stationary state solutions to the DFM and DCCM model. The stationary state DCCM transport equations for a single component system expressed in terms of intrinsic properties for the solute species in the fracture and matrix have the form

$$-\tau_\alpha\phi_\alpha D\frac{d^2C_\alpha}{dx^2} + v_f\frac{dC_\alpha}{dx} = -k_\alpha(C_\alpha - C_{\rm eq}) + (1-2\delta_{f\alpha})\frac{\gamma}{\epsilon_\alpha}(C_f - C_m), \tag{3.1}$$

where the Kronecker delta function $\delta_{f\alpha} = 1$ if $\alpha = f$, and zero otherwise, and the fracture-matrix coupling term γ is defined by

$$\gamma = \frac{(\tau\phi D)_f (\tau\phi D)_m}{d_f(\tau\phi D)_m + d_m(\tau\phi D)_f} \mathcal{A}_{fm}, \tag{3.2}$$

where the notation $d_f = \delta$ and $d_m = l/2$ is introduced to refer to the perpendicular distances from the fracture and matrix node centers, respectively, to their common interface. The kinetic rate constants k_α are effective rate constants equal to the product of the intrinsic rate constant times the specific surface area for the fracture and matrix continua, respectively. Thus they may differ significantly from each other. The coupling term is presumed to be linear in the difference in fracture and matrix concentrations at each node. The coupling strength γ has the same units as the kinetic rate constants [s^{-1}].

At large distances from the inlet the solute concentration approaches the equilibrium concentration C_{eq} of the solid. The transport equations are subject to the following boundary conditions at the inlet and outlet to the fractured porous medium

$$C_\alpha(0) = C_\alpha^0, \quad C_\alpha(\infty) = C_{\text{eq}}. \tag{3.3}$$

To solve the stationary state transport equations, first note that the fracture transport equation may be solved for the matrix concentration C'_m to give

$$C'_m = \left(1 + \frac{\epsilon_f k_f}{\gamma}\right) C'_f + \frac{\epsilon_f v_f}{\gamma} \frac{dC'_f}{dx} - \frac{\epsilon_f (\tau\phi D)_f}{\gamma} \frac{d^2 C'_f}{dx^2}, \tag{3.4}$$

where

$$C'_\alpha = C_\alpha - C_{\text{eq}}. \tag{3.5}$$

Substituting this expression into the matrix transport equation results in the following fourth order ordinary differential equation with constant coefficients

$$a(\gamma)\frac{d^4 C'_f}{dx^4} - b(\gamma)\frac{d^3 C'_f}{dx^3} + c(\gamma)\frac{d^2 C'_f}{dx^2} + d(\gamma)\frac{dC'_f}{dx} + e(\gamma) C'_f = 0. \tag{3.6}$$

The coefficients $a(\gamma)$, $b(\gamma)$, $c(\gamma)$, $d(\gamma)$, and $e(\gamma)$ are defined by

$$a(\gamma) = \frac{\epsilon_f \epsilon_m (\tau\phi D)_f (\tau\phi D)_m}{\gamma}, \tag{3.7a}$$

$$b(\gamma) = \frac{\epsilon_m \epsilon_f}{\gamma}\left(v_m(\tau\phi D)_f + v_f(\tau\phi D)_m\right), \tag{3.7b}$$

$$c(\gamma) = \frac{\epsilon_f v_f \epsilon_m v_m}{\gamma} - \epsilon_m(\tau\phi D)_m\left(1 + \frac{\epsilon_f k_f}{\gamma}\right) - \epsilon_f(\tau\phi D)_f\left(1 + \frac{\epsilon_m k_m}{\gamma}\right), \tag{3.7c}$$

$$d(\gamma) = \epsilon_m v_m\left(1 + \frac{\epsilon_f k_f}{\gamma}\right) + \epsilon_f v_f\left(1 + \frac{\epsilon_m k_m}{\gamma}\right), \tag{3.7d}$$

$$\begin{aligned} e(\gamma) &= \gamma\left[\left(1 + \frac{\epsilon_f k_f}{\gamma}\right)\left(1 + \frac{\epsilon_m k_m}{\gamma}\right) - 1\right], \\ &= \frac{\epsilon_f k_f \epsilon_m k_m}{\gamma} + \epsilon_f k_f + \epsilon_m k_m. \end{aligned} \tag{3.7e}$$

The most general solution to Eqn.(3.6) for an infinite system subject to the boundary conditions at the inlet and outlet given by Eqns.(3.3) has the form

$$C_f(x;\,\gamma) \;=\; Ae^{-q_1 x} + Be^{-q_2 x} + C_{\rm eq}, \tag{3.8}$$

where $q_1(\gamma)$ and $q_2(\gamma)$ are the two nonnegative roots of the characteristic fourth order polynomial

$$p(q;\,\gamma) \;=\; a(\gamma)q^4 + b(\gamma)q^3 + c(\gamma)q^2 - d(\gamma)q + e(\gamma) \;=\; 0. \tag{3.9}$$

Because the coefficient $e(\gamma)$ is positive, there must always exist an even number of positive roots. Because $d(\gamma) \geq 0$, there can be only two nonnegative roots. From Eqn.(3.4), the matrix concentration has the form

$$C_m(x) \;=\; w_1 A_1 e^{-q_1 x} + w_2 A_2 e^{-q_2 x} + C_{\rm eq}, \tag{3.10}$$

where

$$w_i \;=\; 1 + \frac{\epsilon_f k_f}{\gamma} - \frac{\epsilon_f v_f}{\gamma} q_i - \frac{\epsilon_f \tau_f \phi_f D}{\gamma} q_i^2, \quad (i = 1,\, 2). \tag{3.11}$$

The coefficients A_i are related to the boundary conditions imposed on the solution with the values

$$A_i \;=\; (-1)^{i+1} \frac{(C_m^0 - C_{\rm eq}) - w_{3-i}(C_f^0 - C_{\rm eq})}{w_1 - w_2}, \quad (i = 1,\, 2). \tag{3.12}$$

In the limit $\gamma \to 0$ the coupling term vanishes and the matrix and fracture continua evolve independently of one another. The ECM is retrieved in the limit $\gamma \to \infty$.

Stationary state profiles for fracture and matrix concentrations are illustrated in Figure 5 based on the analytical solution for a single component system. A fracture aperture of 1 mm, Darcy flow velocity of 1000 m y^{-1}, matrix block size of 0.1 m, and matrix porosity of 0.05 are used in the calculations. As can be seen from Figure 5(a), as the fracture-matrix surface area increases the matrix concentration plateau decreases. The ECM limit is recovered with increasing time. As shown in Figure 5(b) as the fracture kinetic rate constant increases the ECM limit is obtained at earlier times.

Comparing the stationary state solution for the DCCM formulation, Eqns.(3.8) and (3.10), with the DFM solution given by Eqns.(2.10) and (2.11), very different behavior for the solute concentration is obtained. In particular, a scaling relation between fracture and matrix concentrations does not exist in the DCCM formulation—if for no other reason that there is only one matrix node for each fracture node. In fact, the DFM, DCCM model, and ECM can only agree with each other when the ECM is valid. In the DCCM approach concentration gradients are parallel to the fracture, whereas in the DFM (and DCDM) matrix gradients are perpendicular to the fracture. Although gradients parallel to the fracture could have been included in the DFM, they would not have made a significant difference in the qualitative behavior of the solution for sufficiently rapid fracture flow.

4 NUMERICAL IMPLEMENTATION

4.1 Integrated Finite Volume

To develop numerical techniques for solving the partial differential equations arising from the various formulations of the DCM, it is convenient to use an unstructured grid approach. In this

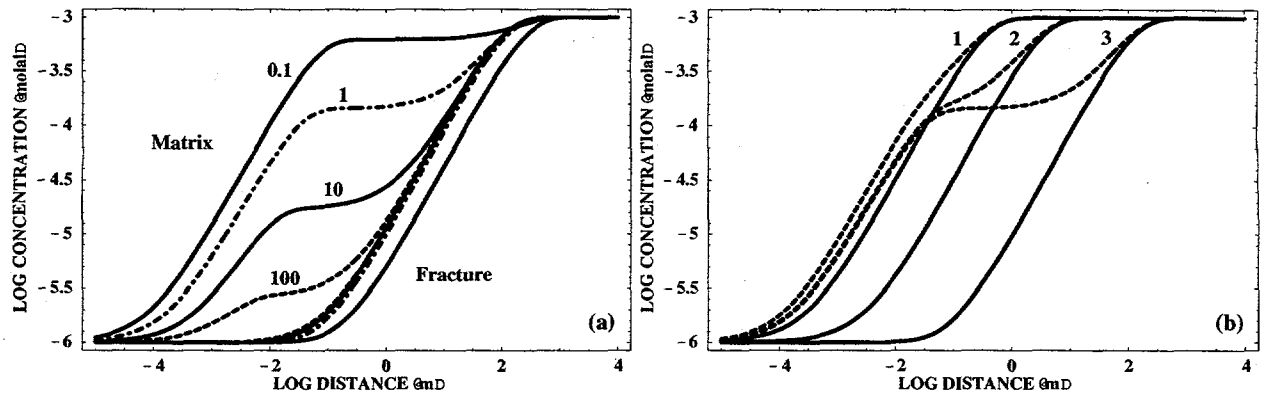

Figure 5: Stationary state concentration profiles based on the analytical solution to the stationary state transport equations. (a) Fracture-matrix surface area multiplied by factors of 100 (dashed), 10 (solid), 1 (dot-dashed), and 0.1 (solid). (b) Fracture (solid) and matrix (dashed) concentration profiles for kinetic rate constant equal to (1) 10^{-10}, (2) 10^{-11}, and (3) 10^{-14} moles cm^{-2} s^{-1}.

approach, nodal connectivity, volumes, distances between connecting nodes, and surface areas can be specified arbitrarily as illustrated in Figure 6 for a simple structured grid geometry with unequal spacing. The integrated finite volume equations for the primary species are expressed simply as

$$\frac{(\tau_n \phi_n \Psi_{jn})_{t+\Delta t} - (\tau_n \phi_n \Psi_{jn})_t}{\Delta t} + \sum_{n'} \mathcal{A}_{<n'n>} \Omega^{t+\Delta t}_{j<n'n>} = -\sum_s \nu_{js} I^{t+\Delta t}_{sn}, \tag{4.1}$$

for a fully implicit time discretization with time step Δt. The flux $\Omega_{j<n'n>}$ is defined as

$$\Omega_{j<n'n>} = -(\tau\phi D)_{<n'n>} \frac{\Psi_{jn} - \Psi_{jn'}}{d_n + d_{n'}} + v_{<n'n>} \Psi_{j<n'n>}. \tag{4.2}$$

The notation $<n'n>$ refers to the interface between nodes n and n' with interfacial area $\mathcal{A}_{<n'n>}$ and distances to the interface denoted by d_n and $d_{n'}$. The sum in Eqn.(4.1) is over all which are nodes connected to the nth node. Note that there is no reference to fracture or matrix properties as that is handled automatically by the grid structure and its connectivity. Even explicit reference to the fracture-matrix coupling term has disappeared in the integrated finite volume form of the equations which is now included in the term containing the sum over fluxes. This approach offers greater flexibility in programming both the DCCM and DCDM methods, requiring only a change in preprocessor to invoke the appropriate geometrical relation between nodes. The internal part of the code can remain the same.

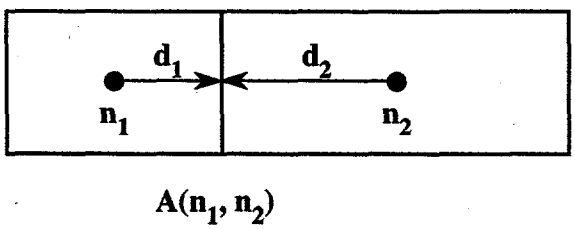

Figure 6: Integrated finite volume geometry.

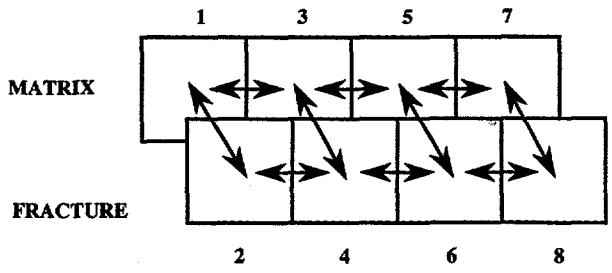

Figure 7: Nodes and their connections for the DCCM model.

Table 2: Node connections for the DCDM model with grid numbering as shown in Figure 4.

Node	Connecting Nodes			
1	1	2	7	
2	1	2	3	
3	2	3	4	
4	3	4	5	
5	4	5	6	
6	5	6		
7	1	7	8	13
8	7	8	9	
9	8	9	10	
...		...		

Examples of integrated finite volume grids for the DCDM and DCCM formulations are illustrated in Figures 4 and 7, respectively. Note that the DCCM grid is in fact just a two-dimensional (2D) problem with two y-nodes. The difference between a true 2D problem and the DCCM grid, lies in the different assignment of areas at the fracture-matrix interface. The node connections for the DCDM model corresponding to Figure 4 are listed in Table 2.

The flexibility of the unstructured grid framework of the various dual continuum formulations allows for practically arbitrary assignment of block connections and surface areas. However, one must ensure that the resulting finite volume equations actually represent partial differential equations. It is important to be certain that the processes to be modeled can actually take place physically and are not merely an artifact of some artificially imposed grid structure.

4.2 DCCM: Harmonic Versus Arithmetic Averaging

An important consideration in the numerical implementation of the DCCM model is the computation of interface properties between fracture and matrix. This is especially true because of the often great difference in fracture aperture and matrix block size. In finite difference form the coupling term Eqn.(2.27) is given by

$$\Gamma_j^{fm} = \mathcal{A}_{fm}(\tau\phi D)_{fm}\frac{\Psi_j^f - \Psi_j^m}{d_f + d_m}, \tag{4.3}$$

where as previously defined following Eqn.(3.2), $d_f = \delta$ and $d_m = l/2$. To evaluate the product $\tau\phi D$ at the fracture-matrix interface, harmonic or arithmetic averages are possible. The harmonic average is more rigorously based from considerations of the steady-state flux across the interface (Patankar, 1980). For $d_f \ll d_m$, the harmonic mean yields

$$(\phi\tau D)_{fm}^{\text{harm}} = \frac{(d_f + d_m)\,(\tau\phi D)_f(\tau\phi D)_m}{d_m(\tau\phi D)_f + d_f(\tau\phi D)_m} \simeq (\tau\phi D)_m. \tag{4.4}$$

Thus the harmonic mean yields a coupling term proportional to the effective matrix diffusivity. The arithmetic mean, however, gives for the interface property

$$(\phi\tau D)_{fm}^{\text{arith}} = \frac{d_m(\tau\phi D)_f + d_f(\tau\phi D)_m}{d_m + d_f} \simeq (\tau\phi D)_f, \tag{4.5}$$

yielding a coupling term proportional to the effective fracture diffusivity. Because the intrinsic fracture porosity ($\phi_f \sim 1$) is generally much larger than the matrix porosity ($\phi_m \ll 1$), harmonic averaging leads to a smaller coupling term compared to arithmetic averaging. Which approach is correct? Intuitively, one would expect that the flux across the fracture-matrix interface would be governed by diffusion in the matrix and not the fracture, because of the very small fracture aperture, and hence harmonic averaging is preferred.

The DCCM model appears to give the incorrect behavior as the matrix block size is increased. Evaluating the coupling term Eqn.(2.27) using harmonic averaging according to Eqn.(4.4) and inserting Eqn.(2.28) for the interfacial area, it is apparent from the finite difference form of the coupling term Eqn.(4.3) that as the matrix block size increases, the coupling term decreases as d_m^{-2}

$$\Gamma_j^{fm} \sim (1-\epsilon_f)\frac{(\tau\phi D)_m}{d_m^2}\left(\Psi_j^f - \Psi_j^m\right). \tag{4.6}$$

As a consequence, coupling between fracture and matrix decreases as the matrix block size increases. This behavior runs counter to that predicted by the DFM and what intuitively is to be expected. That is, the fracture-matrix interaction should be independent of the matrix block size, at least for times which are short compared to the transport time across the matrix block. The DCDM model does not have this limitation and is able to describe narrow alteration halos surrounding fractures resulting from sharp concentration gradients within the rock matrix.

Numerical difficulties arise when applying the DCCM model to cases where the fracture volume fraction ϵ_f is very small. As shown in Figure 8, variable grid spacing can lead to completely erroneous results for mineral concentrations. In this figure, the DCCM model is applied to formation of kaolinite resulting from the alteration of K-feldspar. Results are compared for uniform and variable grid spacing using harmonic averaging. Each pair of curves compare uniform grid spacing with a change in spacing at 0.5 m from the inlet. Grid spacing varies from 0.0075 m to 0.09 m as indicated in the figure. As can be seen from the figure, an erroneous jump in the kaolinite volume fraction is obtained at a change in grid spacing. The magnitude of the jump is also very sensitive to the absolute grid size. The DCDM model, on the other hand, does not suffer from this difficulty since a small grid spacing on the order of the fracture aperture can used to discretize the matrix in the neighborhood of the fracture.

4.3 DCDM: Decoupling Fracture and Matrix Transport Equations

Computationally, the DCDM model is generally much more expensive compared to the DCCM model. For a spatial domain consisting of N_f fracture nodes and N_m nodes within each matrix block, for an N_c component system the DCDM model requires solving $N_c \times N_f \times N_m$ simultaneous equations; whereas the DCCM model requires solving only $2 \times N_c \times N_f$ equations. However, perhaps surprisingly, it is possible to rigorously decouple the fracture and matrix equations in the DCDM model reducing the system of equations to $N_c \times (N_f + N_m)$ in number. As noted by Gilman (1986) this is possible because of the one-dimensional form of the matrix equations in the DCDM model. This result is surprising given the strong, nonlinear, coupling that is possible between fracture and matrix continua. The procedure outlined by Gilman (1986) involves first a backward solution of the matrix equations beginning with the inner most matrix node. This provides a relation between the concentration at outer most matrix node and the concentration at the adjacent fracture node. With this result the matrix concentration appearing in the coupling term in the fracture equations can be eliminated. As a result, the fracture equations are only a function of the fracture concentration and may be solved independently of the matrix equations. Once the fracture equations are solved, the solution of the matrix equations can be completed through a forward sweep of the matrix

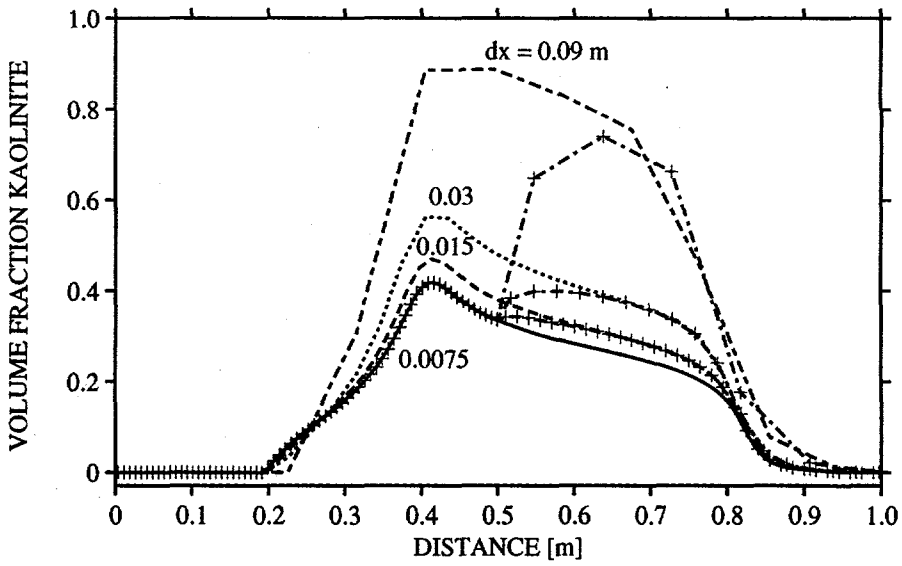

Figure 8: Profiles showing the volume fraction of Kaolinite which precipitates as K-feldspar is weathered. Shown are profiles for different grid spacing based on the harmonic mean. The calculations correspond to an elapsed time of 10,000 years with a fracture flow rate of 1000 m y^{-1} and fracture volume fraction $\epsilon_f = 10^{-3}$. The intrinsic fracture porosity is unity and matrix porosity 0.1.

nodes beginning with the outer most node. This approach also lends itself to parallel computing techniques (Seth and Hanno, 1995; Smith and Seth, 1999) in which the matrix equations can be solved in parallel, greatly reducing computation times and dramatically extending the capability of the DCDM to much larger numbers of nodes and chemical components that could be solved without these techniques.

5 EXAMPLE: *IN SITU* COPPER LEACHING

To illustrate and contrast the various approaches previously discussed for describing transport in porous fractured media, an example problem of *in situ* leaching of a hypothetical copper ore body is presented (Lichtner, 1998). Calculations were carried using the computer code FloTran (Lichtner, 1999). A one-dimensional column is considered containing the copper-bearing phase chrysocolla and gangue minerals in the form of kaolinite and quartz. A sulfuric acid solution with pH 1 is allowed to infiltrate into the column through a fracture network. The initial fluid in the column is assumed to be in equilibrium with chrysocolla, kaolinite, and quartz at a pH of 8. The composition of the host rock for the model ore deposit is listed in Table 3. For the model parameters listed in the table, the ore body has a copper grade of 0.90% and bulk rock density of approximately 2.44 g cm^{-3}. A matrix block size of 0.1 m is used in the calculations. A fracture aperture of 1 mm corresponding to a fracture volume fraction of $\epsilon_f = 2.941 \times 10^{-2}$ is used. A bulk Darcy velocity of 10 m y^{-1} corresponding to a fracture velocity of 340.02 m y^{-1}, and an effective matrix diffusivity of 10^{-6} cm^2 s^{-1} is used in the calculations. In the DFM and DCDM model, the matrix was discretized into 10 grid blocks of variable spacing with the smallest spacing equal to the fracture aperture neighboring the fracture. Secondary minerals which form during leaching are amorphous silica, gypsum, jurbanite, and alunite, and secondary copper minerals brochantite and antlerite.

Results for the copper breakthrough curves for the different models are shown in Figure 9. If

Table 3: Model ore deposit giving primary ore and gangue mineral abundances, porosities, and associated mineral surface areas used in the calculations for dual, equivalent, and single continuum models. Values for the SCM are bulk properties.

	Volume Fraction				Surface Area [cm^{-1}]			
Property	Fracture	Matrix	ECM	SCM	Fracture	Matrix	ECM	SCM
Chrysocolla	0.2	0.02	0.0253	0.0059	42.	4.	5.118	1.235
Quartz	0.0	0.73	0.7085	0.	1	14.6	1	0.0294
Kaolinite	0.0	0.2	0.1941	0.	1	40.	38.82	0.0294
Porosity	0.8	0.05	0.0721	0.0235				

diffusion is turned off, then the assumption no flow in the matrix would require that the SCM must give identical results as the DCCM and DCDM models. Thus differences between breakthrough curves for these models are due to differences in how the interaction term between fracture and matrix is treated. The SCM breakthrough curve exhibits a single peak resulting from dissolution of chrysocolla in the fractures. Likewise the ECM also exhibits a single peak but which is delayed in time compared to the SCM as expected from Eqn.(2.49) which predicts a retardation of approximately

$$1 + \frac{\epsilon_f \phi_f}{\epsilon_m \phi_m} \simeq 3.02, \tag{5.1}$$

in agreement with the figure.

The width of the ECM peak is longer compared to the SCM since there is more copper to dissolve because the ECM incorporates copper from both the rock matrix and fractures. The breakthrough curves for the DFM and DCCM and DCDM models, show a bimodal distribution resulting from contributions from individual fracture and matrix copper sources. The shapes of the curves are somewhat different with the DCDM model agreeing more closely with the DFM. Differences between the DFM and DCDM model can be attributed to different formulations of the matrix which is treated as three-dimensional cubical blocks in the DCDM. The DCCM curve follows closely to the SCM result during the early part of breakthrough dominated by dissolution of copper in fractures, but then drops off to an almost constant value as the matrix becomes the dominant contributor. Clearly, the DCCM model is unable to give the proper behavior at longer times and overshoots the copper concentration as predicted by the DFM and DCDM model at early times.

It should be noted that the peak copper concentration is quite high in these simulations compared to what might be expected from an actual five spot leach field. This is an artifact of the one-dimensional form of the calculations.

6 CONCLUSION

Describing quantitatively reactive flow and transport in fractured porous media presents a number of challenges that have yet to be resolved satisfactorily. Dual continuum models attempt to account for the bimodal distribution in physical and chemical properties characteristic of fractured porous media. An equivalent porous medium description is generally unable to capture the unique features characteristic of fractured systems. Dual continuum models are presumably applicable to highly fractured systems where the DFM becomes impractical, but not so highly fractured that the system can be described as a equivalent continuum. Whether a dual continuum as opposed to a single

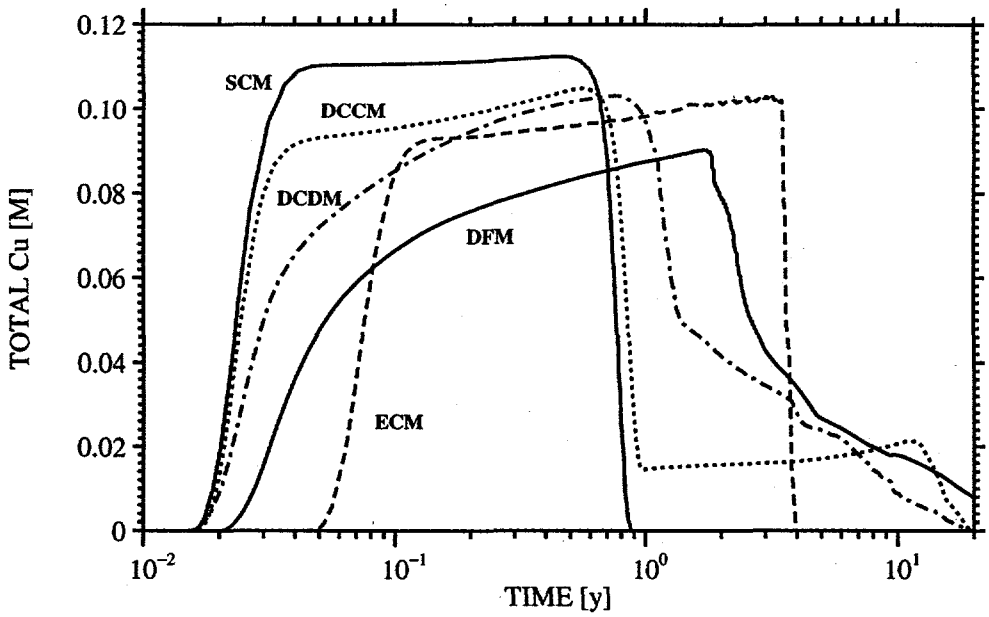

Figure 9: Copper breakthrough curves for the SCM, ECM, DFM, DCCM and DCDM models.

continuum representation of the fracture network only is appropriate, depends on the time scales of interest and the extent of interaction between the fracture network and rock matrix.

Two different DCM models were discussed in detail, characterized by the connectedness of the rock matrix. In the DCCM model, the matrix formed a connected continuum with each fracture node associated with a single matrix node. The validity of the DCCM model rests on the absence of strong concentration gradients within the matrix perpendicular to the fracture. This is a consequence of representing the matrix by a single node for each fracture node. The DCCM model should be applicable to situations where the kinetic reaction rate varies smoothly over the matrix block, or equivalently, the characteristic chemical equilibration length scale is long compared to the matrix block size. Faster reactions imply shorter equilibration length scales, leading to steeper gradients, and eventually failure of the DCCM approach.

An alternative approach, the DCDM model, is applicable to situations where the fracture network segregates the matrix into disconnected blocks which can only communicate with one another through their common fracture interface. Within each matrix block, a fine grid may be used to capture arbitrarily sharp gradients, thereby eliminating one of the limitations of the DCCM model. However, in contrast to the DCCM approach, the DCDM model associates a single fracture node with each matrix block which completely surrounds the block. This symmetry imposes severe constraints on the DCDM model. It is not possible, for example, to account for gradients or reaction fronts across matrix blocks arising, for example, from gravity driven flow. Furthermore, incorporation of heterogeneous matrix blocks would destroy this symmetry. Finally, it does not appear possible to describe simultaneous heat and mass flow within the DCDM framework.

Many conceptual difficulties remain in providing a quantitative description of reactive flow and transport in fractured porous media. Although not discussed in any detail here, especially difficult is obtaining the necessary data to apply the models to a particular field situation. Both the DCCM and DCDM approaches introduce additional parameters such as matrix block size, fracture aperture, and fracture-matrix interaction parameters, which represent averages over distributions and which are difficult to measure and characterize. In addition, these models require characterizing the reactive surface area of minerals separately for fracture and matrix continua from experimental and field data.

7 ACKNOWLEDGMENTS

The author would like to thank Rajesh Pawar and Daniel Tartakovsky for helpful discussions on this topic, and Tianfu Xu, Joel VanderKwaak, Daniel Tartakovsky, and an anonymous reviewer for reviewing the manuscript.

8 REFERENCES

Abdassah, D. and Ershaghi, I. (1986) SPE Form. Eval. 1, 113.

Bai, M., D. Elsworth, J.-C. Roegiers (1993) Multiporosity/multipermeability approach to the simulation of naturally fractured reservoirs, Water Resour. Res., 29, 1621-1633.

Barenblatt, G.I. and Iu.P. Zheltov (1960) Fundamental equations of filtration of homogeneous liquids in fissured rocks, Soviet Physics–Doklady, 5, 522-525.

Barenblatt, G.I., Iu.P. Zheltov, and I.N. Kochina (1960) Basic conceptions the theory of seepage of homogeneous liquids in fissured rocks, J. Appl. Math. Mech., 24, 1286–1303.

Chen, Z.-X. (1989) Trans. Porous Media, 4, 147.

Chittaranjan, R., Ellsworth, T.R., Valocchi, A.J., and Boast C.W. (1997) An improved dual porosity model for chemical transport in macroporous soils, J. Hydro., 193, 270–292.

Closmann, P.J. (1975) Soc. Pet. Eng. J. 15, 385.

Gerke, H.H., and M.T. Van Genuchten (1993) A dual porosity model for simulating the preferential movement of water and solutes in structured porous media, 29, 305–319.

Gilman, J.R. (1986) An efficient finite-difference method for simulating phase segregation in the matrix blocks in double-porosity reservoirs. SPERE, July, 403–413.

Hill, A.C., and G.W. Thomas (1985) A new approach for simulating complex fractured reservoirs. SPE 13537, 429–436.

Lichtner P.C. (1985) Continuum model for simultaneous chemical reactions and mass transport in hydrothermal systems, Geochimica et Cosmochimica Acta, 49:779–800.

Lichtner, P.C. (1988) The quasi-stationary state approximation to coupled mass transport and fluid-rock interaction in a porous media. Geochimica et Cosmochimica Acta, 52, 143–165.

Lichtner, P.C. (1993) Scaling properties of time-space kinetic mass transport equations and the local equilibrium limit. American Journal of Science, 293, 257–296.

Lichtner, P.C. (1998) Modeling reactive flow and transport in natural systems, Eds. G. Ottonello and L. Marini, Environmental Geochemistry, Pacini Editore, Pisa, Italy, 5–72.

Lichtner, P.C. (1999) FloTran User's Manual. In preparation.

Lichtner, P.C., and M.S. Seth (1996) Multiphase-multicomponent nonisothermal reactive transport in partially saturated porous media: Application to the Proposed Yucca Mountain HLW Repository; Proceedings International Conference on Deep Geologic Disposal of Radioactive Waste. Canadian Nuclear Society, September 16-19, Winnipeg, Manitoba, Canada. 3-133–3-142.

Lichtner, P.C., Steefel, C.I., and Oelkers, E.H. (Eds.) (1996) Reactive transport in porous media. Reviews in Mineralogy, 34, 438 pp.

Odling, N.D., J.E. Roden (1997) Contaminant transport in fractured rocks with significant matrix permeability, using natural fracture geometries, J. Contaminant Hydrology, 27, 263-283.

Patankar, S.V. (1980) Numerical Heat Transfer and Fluid Flow, Hemisphere Series on Computational Methods in Mechanics and Thermal Science, 197 p.

Pruess, K. and Narisimhan, T.N. (1985) A practical method for modeling fluid and heat flow in fractured porous media. Soc. Pet. Eng., 25, 14-26.

Seth, M.S., and Hanano, M. (1995) An efficient solution procedure for multiple interacting continua flow. Proc. of World Geothermal Congress. Florence, Italy. p. 1625.

Smith, E.H., and Seth, M.S. (1999) Efficient solution method for matrix-fracture flow with multiple interacting continua. Int. J. Numer. Anal. Meth. Geomech., 23, 427–438.

Steefel, C.I. and Lichtner, P.C. (1998a) Multicomponent Reactive Transport in Discrete Fractures: I. Controls on Reaction Front Geometries, J. Hydrology, 209, 186–199.

Steefel, C.I. and Lichtner, P.C. (1998b) Multicomponent Reactive Transport in Discrete Fractures: II. Infiltration of Hyperalkaline Groundwater at Maqarin, Jordan, a Natural Analogue Site, J. Hydrology, 209, 200–224.

Thomas, L.K., T.N. Dixon, and R.G. Pierson (1983) Fractured reservoir simulation. SPEJ 9305, 42–54.

Warren, J.E., and P.J. Root (1963) The behavior of naturally fractured reservoirs, Soc. Petrol. Eng. J., 3, 245–255.

Zyvoloski, G.A., Robinson, B.A., Dash, Z.V., and Trease, L.L. (1997) Summary of the models and methods for the FEHM application—A finite-element heat- and mass-transfer code, LA-13307-MS, Los Alamos National Laboratory.